IN-SITU MASS SPECTROSCOPY IN HIGH DENSITY PLASMA ENHANCED CHEMICAL VAPOR DEPOSITION OF SILICON NITRIDE THIN FILMS*

H. Bola George
GLCA/ACM ORSS Program
Coe College
Oak Ridge National Laboratory
Oak Ridge, TN 37831

December 10, 1999

Prepared in partial fulfillment of the requirements of the Great Lakes Colleges Association/Associated Colleges of the Midwest Oak Ridge Science Semester under the direction of Dr. John Caughman, research advisor in the Oak Ridge National Laboratory Fusion Energy Division.

*Research sponsored by the U.S. Department of Energy at ORNL under contract DE-AC05-96OR22464 with Lockheed Martin Energy Research Corporation

IN-SITU MASS SPECTROSCOPY IN HIGH DENSITY PLASMA ENHANCED CHEMICAL VAPOR DEPOSITION OF SILICON NITRIDE THIN FILMS

H. Bola George

ABSTRACT

In-situ mass spectroscopy is used to analyze process conditions and chemistry of atom-molecule kinetics in high density plasma enhanced chemical vapor deposition (PECVD) of silicon nitride thin films. Process conditions are related to film quality by using a quadropole mass spectrometer to monitor the amounts of atomic hydrogen, nitrogen, and silicon radicals in the gas phase. Results - from Hydrogen Forward Scattering (HFS), Rutherford Back Scattering (RBS), and Fourier Transform Infra Red (FTIR) studies - confirm reduced hydrogen incorporation in films, which is linked to the production of atomic hydrogen in the plasma and the likely abstraction of hydrogen from the growing film. In addition, a correlation is made between the silane dissociation pattern in the gas phase and the mechanism for film growth on the substrate surface.

INTRODUCTION

Amorphous hydrogenated silicon nitride (SiN_X:H) thin films have gained widespread attention due to their technological potential to be used in thin film transistors and as waveguide materials, where unique properties such as its mechanical and electronic integrity at high temperatures are especially desirable[1, 2, 3] in the fabrication of high refractive index and optical band gap materials. A novel approach has been developed by scientists[4] at ORNL in which high density radio frequency (rf) inductively coupled discharges are used to provide better deposition rates and reduced hydrogen in films at much lower substrate temperatures (< 400ºC). Various methods[5] have been used in film fabrication but mixtures of SiH_4 with either N_2 or NH_3 in plasma set-ups are the favored, the former being the preferred gas since it introduces less hydrogen in films [6] .

Previous work[7] and our deposition results have shown that hydrogen plays a significant role in altering silicon nitride properties. As a result, the importance of this study is underscored since it uses *in-situ* mass spectroscopy to relate gas phase species, SiH_x (x=1, 2, or 3) to observed film properties. In particular, the following are shown: increased dissociation of hydrogen, nitrogen, and silane are shown to be the cause of the higher deposition rates, and an increase in the atomic hydrogen flux causes reduced hydrogen in films when hydrogen gas is introduced into the plasma chamber. These have been confirmed from recent RBS and FTIR studies. In addition, our results for maximum dissociation of the molecular gases correspond to conditions that yielded best quality films. Also, a correlation of atom-molecule reaction mechanism in film growth is made to the silane consumption pattern. This report is a snapshot of work in progress.

EXPERIMENTAL DETAILS

The ORNL approach to plasma enhanced chemical vapor deposition (PECVD) involves use of an inductively coupled plasma (ICP) source to produce the essential reactive species required for thin film growth. A schematic diagram of the ICP set-up is shown in figure 1. Chamber specifics include a diameter of 30 cm. Gases are introduced into the chamber using gas rings. The gas ring for silane is 10 cm lower than that used for hydrogen or nitrogen which are injected near the plasma excitation region. Compared to capacitively coupled plasma (CCP) discharges that have lower efficiency for atomic species (about 2%) and poor reaction selectivity, ICP sources produce higher dissociation efficiency (20 to 30%) of diatomic species. This arises from the higher plasma densities achievable with ICP reactors. In addition, other advantages of ICPs include increased deposition rates (ten times), decreased substrate temperatures (<400ºC compared to 800ºC in CCPs), and their adaptability for large area manufacturing (> 300 mm diameter). Inherently non-destructive, *in-situ* mass spectroscopy allow analysis of key reactions such as atom-molecule kinetics and intermediate species identity.

The plasma power is controlled by a radio frequency (rf) configuration coupled at 13.56 MHz.

A doubly-differentially pumped quadrupole mass spectrometer (QMS) with a standard ionizer installed in place of the substrate was used to monitor critical process conditions, illustrated in figure 2. Unless stated otherwise, the ionizer energy was set at 70 eV.

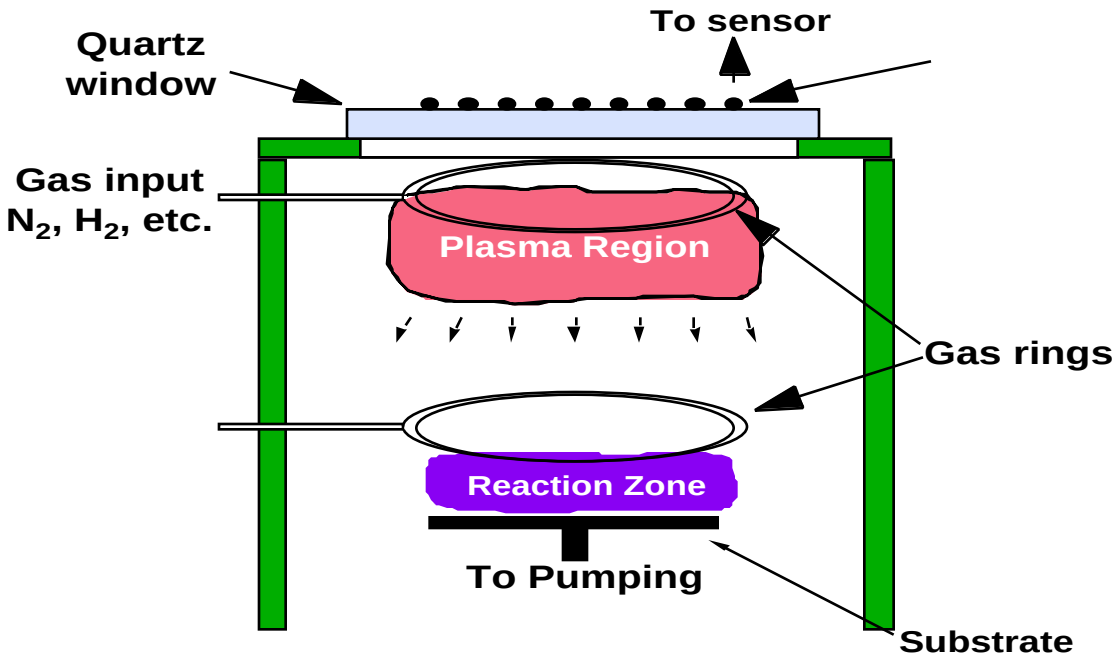

Figure 1: Diagram of inductively coupled plasma discharge used in our experiments

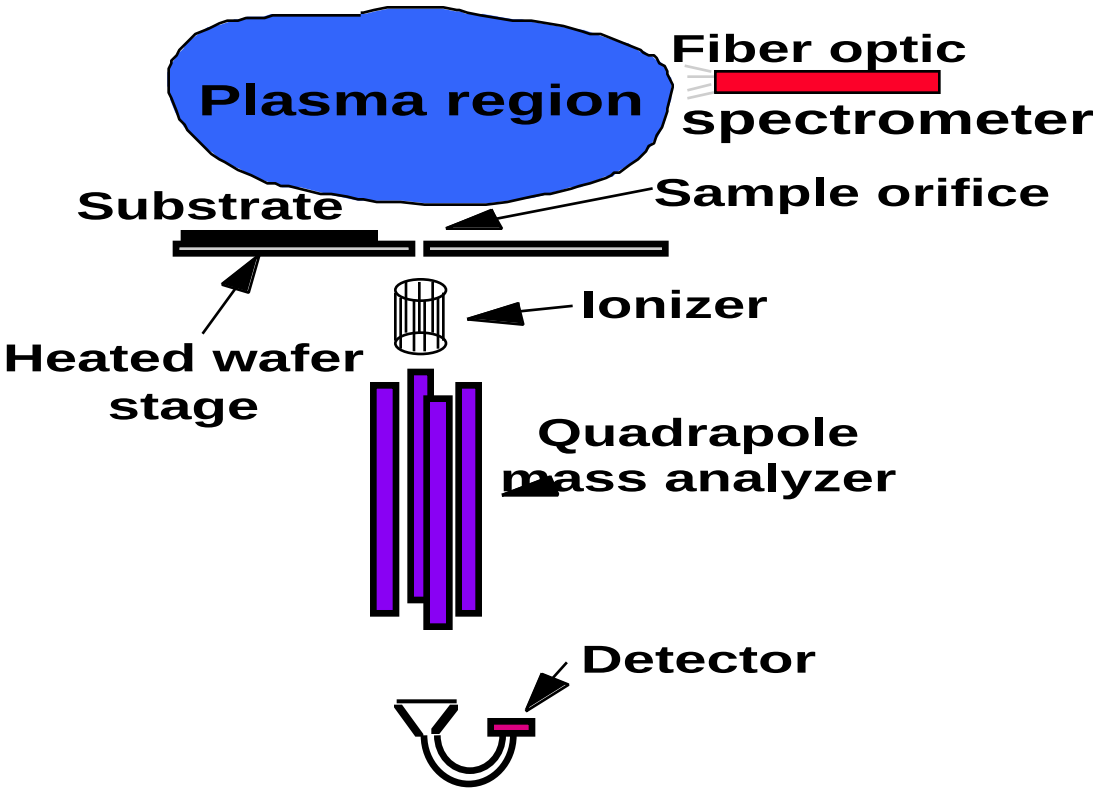

Figure 2: Schematic of quadrupole mass spectrometer used for *in-situ* analysis

Typical experiments were conducted such that 30 second or one minute plasma on-off pulses were recorded as process parameters - power, pressure, gas flow rates, or ionizer energy - were changed. For instance, in a given experiment to monitor the behavior of hydrogen, the throttle valve pressure was fixed at 50 mTorr, while the power was changed from 200 W to 1.5 kW. In cases where silane was used, its flow rate was fixed at 10 standard cubic centimeters per minute (sccm).

Methods used to evaluate the films after depositions included Fourier Transform Infra-Red spectrometry (FTIR) to determine stretching modes, Hydrogen Forward Scattering (HFS) and Rutherford Back Scattering (RBS) measurements for determination of atomic concentrations in the films, and ellipsometry to determine the film thickness and the optical properties such as refractive index and band gap.

RESULTS

Data collected were analyzed using MS Excel® and Kaleidograph® spreadsheets. Analysis involved calculating dissociation for the molecular species and quantifying the SiH_x fragments from silane break-up. Illustrative of raw data collected, figure 3 shows the plasma on-off cycles for the H_2 (mass 2) signal as operating parameters were changed; in this case, corresponding to a fixed hydrogen flow rate (150 sccm) and pressure (50 mTorr) as power was changed. Estimation for a lower dissociation limit is made from the changes in the plasma on-off levels as indicated.

Figures 4 and 5 are dissociation fractions for a hydrogen plasma , with a flow rate of 150 sccm. The former represents collected data at a pressure of 50 mTorr and changing power; the latter is kept at 1250 W as a function of pressure.

Figures 6 and 7 show dissociation for a nitrogen plasma maintained at a flow rate of 50 sccm.

For a nitrogen-silane system in the absence and presence of hydrogen, the consumption of silane is shown in figures 8 and 9. The dissociation was calculated from changes in the m/e 30 signal. For these, the ionizer was maintained at 70 eV.

Figures 10 shows the sensitivity of the SiH^+ fragments as a function of ionizer potential. The mass signals were first normalized by the electron current at a given energy, then expressed as a percentage of the maximum value. Included in the plots are data from previous work[8,9], calculated by normalizing the ionization cross sections at different energies by the maximum cross section (50 and 45 eV respectively).

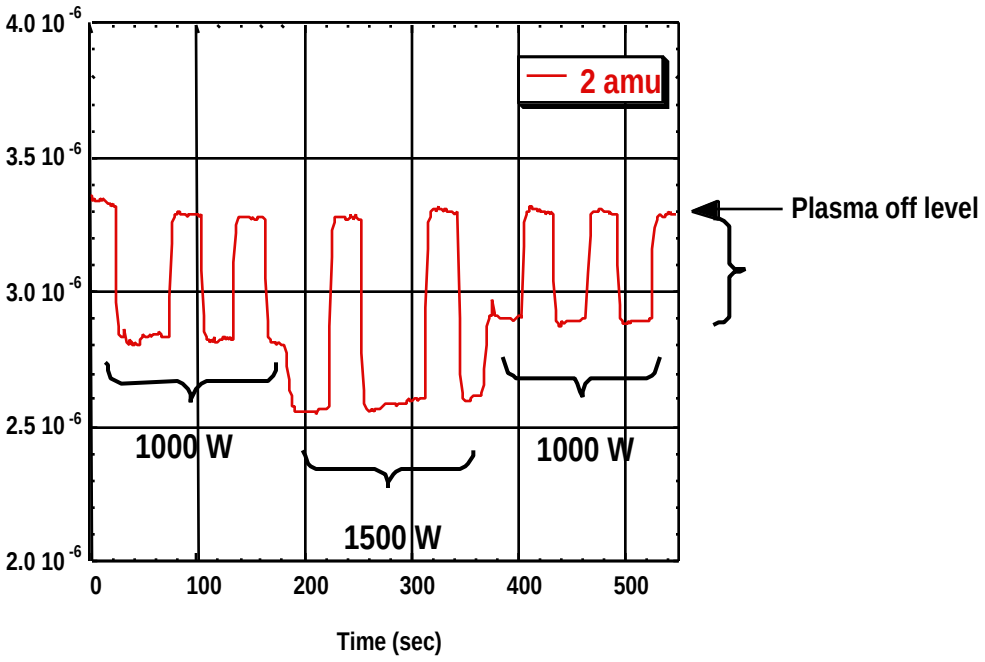
4.0 10 -6
3.5 10 -6
3.0 10 -6
2.5 10 -6
2.0 10 -6
2 amu
Plasma off level
1000 W
1500 W
1000 W
0
100
200
300
400
500
Time (sec)

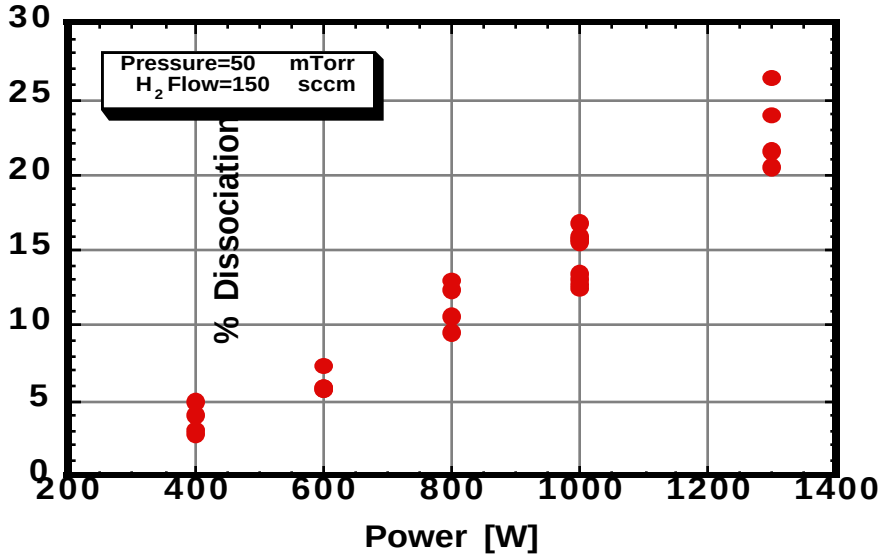

Figure 4: Dissociation of H_2 as a function of power at fixed pressure

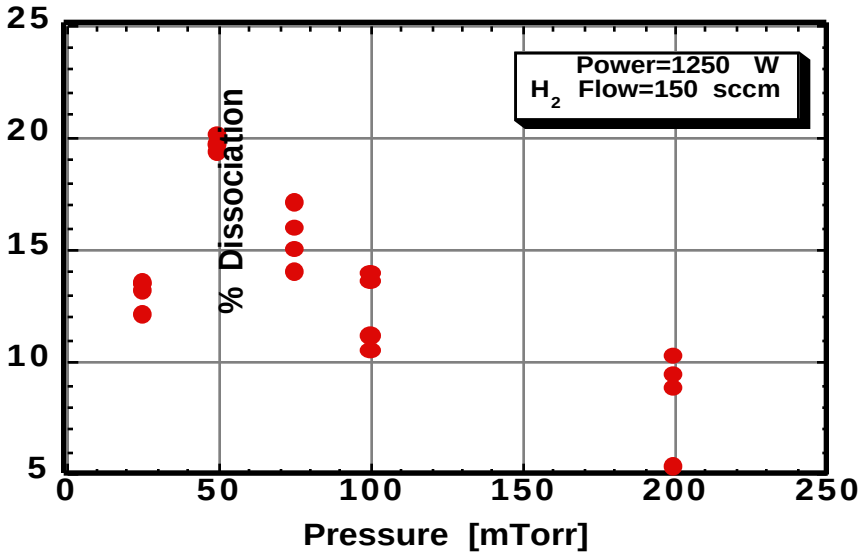

Figure 5: Dissociation of H_2 versus pressure at 1250 W

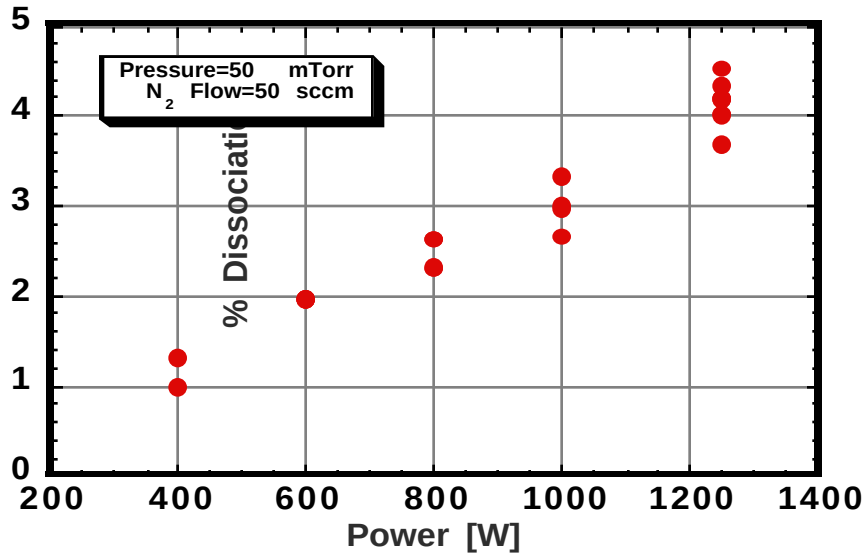

Figure 6: Dissociation of N_2 as a function of power

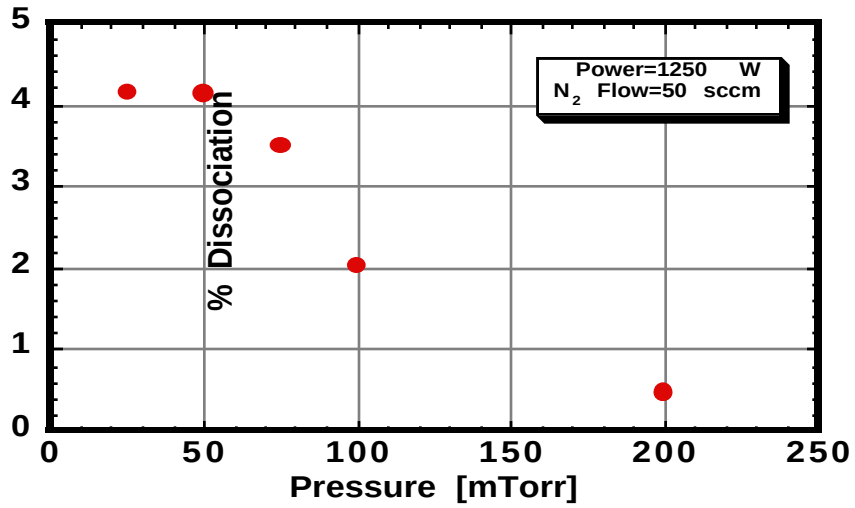

Figure 7: Nitrogen dissociation as function of pressure

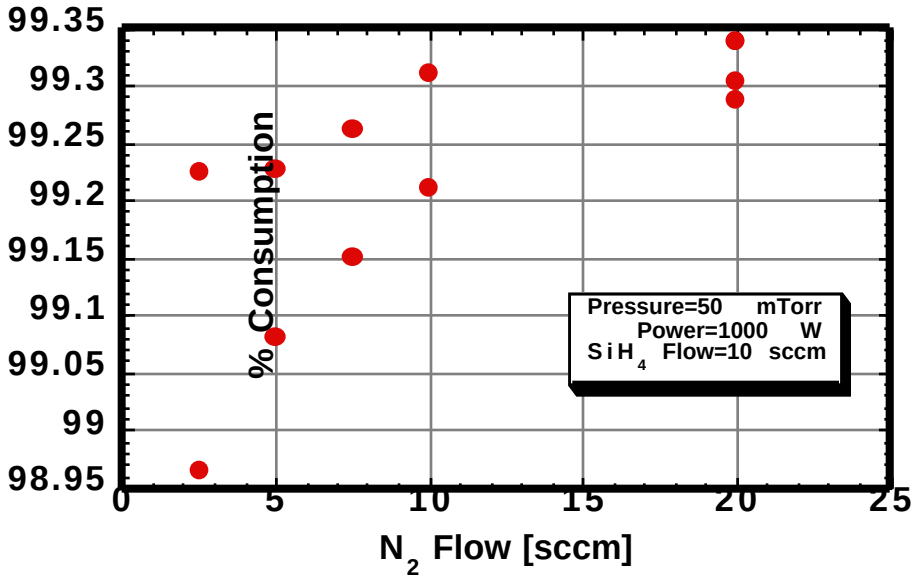

Figure 8: Higher silane consumption in absence of H_2 gas

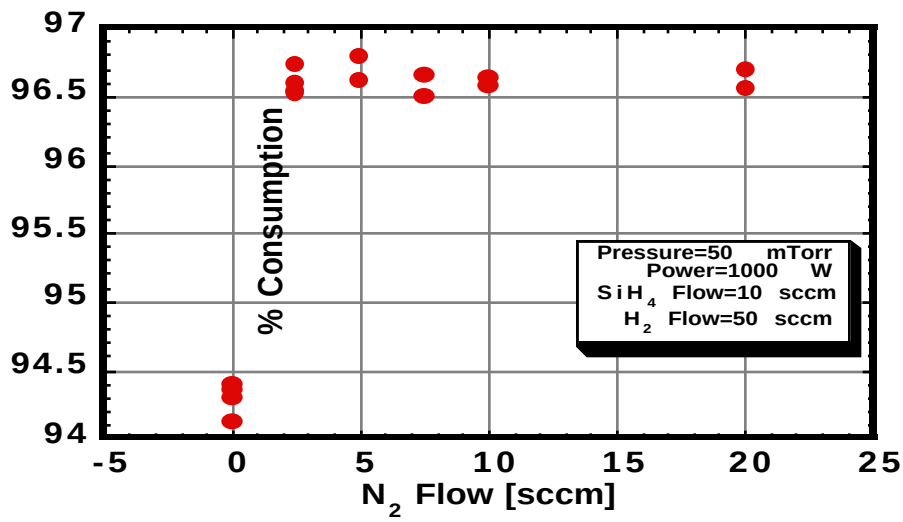

Figure 9: Slightly lower silane consumption with H_2 gas addition

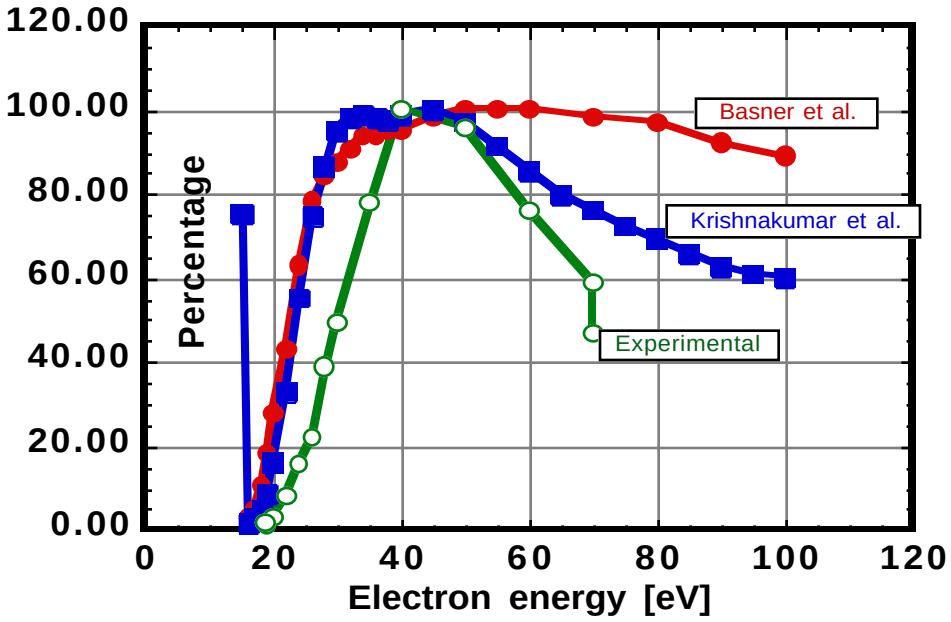

Figure 10: Normalized SiH^+ w.r.t. its max value

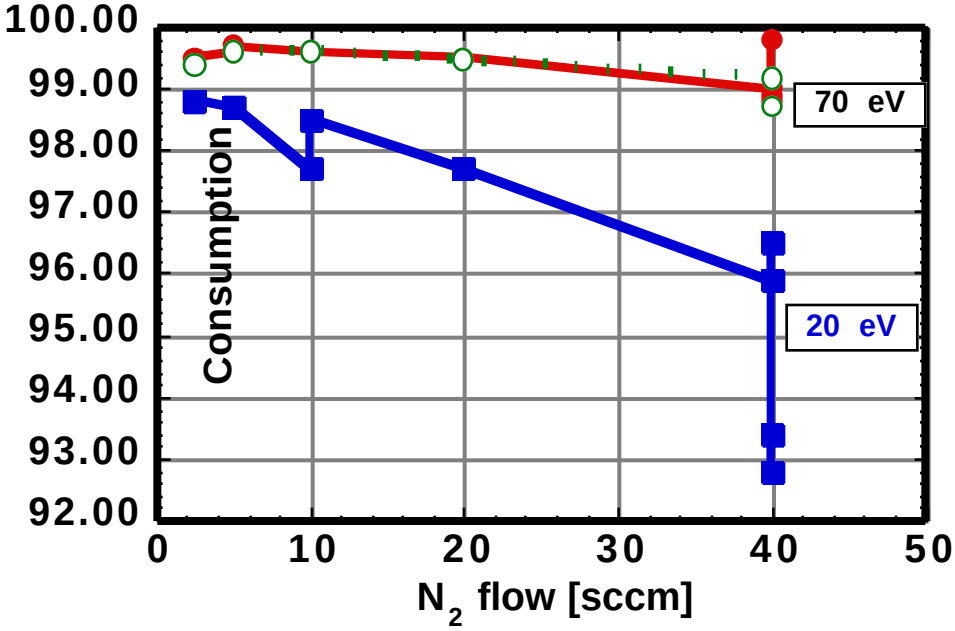
100.00
99.00
98.00
97.00
96.00
95.00
94.00
93.00
92.00
Consumption
0
10
20
30
40
50
N2 flow [sccm]
70 eV
20 eV

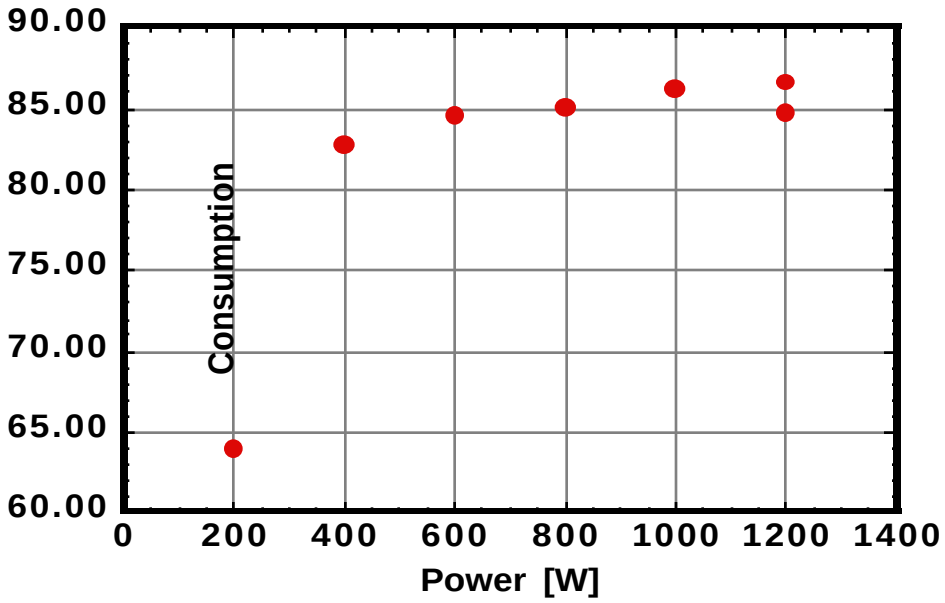

Figure 13: Change in SiH_2 signal at 20 eV in silane-hydrogen plasma

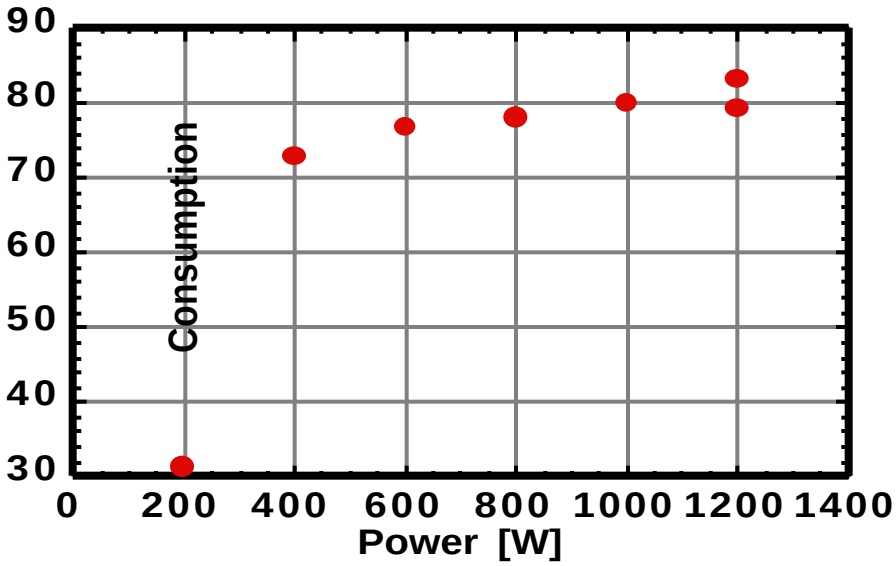

Figure 14: Change in SiH_2 signal at 70 eV in silane-hydrogen plasma

DISCUSSION/RESULTS ANALYSIS

Hydrogen dissociation is related to the production of atomic hydrogen by the equation,

(1) $H_2 \rightarrow H + H$ 4.52 eV

Shown in figures 4 and 5, hydrogen dissociation increases with power and peaks at 50 mTorr, consistent with most deposition being centered around 50 mTorr for best film quality. Recycling and recombination at the chamber surfaces has the effect of increasing the hydrogen signal when the plasma is on, that is, the surfaces also act as a source of H_2. A peak at 656.1 nm corresponding to H-alpha (H_α) has been observed from the OES spectra. Similarly, the nitrogen dissociation shown in (2) increases with power and again attains a maximum around 50 mTorr.

(2) $N_2 \rightarrow N + N$ 9.81 eV

By comparing figures 4 to 7, it is seen that nitrogen dissociation is less than hydrogen. This can be explained on the basis of nitrogen having a higher bond energy, 9.81 eV as opposed to 4.52 eV for hydrogen.

Silane consumption is high for our processing conditions. The high density plasma breaks up the silane in both absence and presence of hydrogen, figures 8 and 9. Again, this explains the higher flux of atomic species that are responsible for higher deposition rates compared to other conventional deposition techniques using CCP discharges in which silane consumption is between 30 and 60%. This leads to another drawback of conventional methods. Since the energy of the impinging ions are tied to the plasma

power, higher plasma densities usually imply higher ion energies which are not desirable due to their ability to penetrate and destroy substrate surface. Conversely, in ICP discharges, ion energies and plasma power are decoupled, implying high densities can be attained with relatively low ion energies.

A number of experiments[8, 9, 10, 11, 12] have been performed to determine the sensitivity of the SiH^+ and SiH_3^+ ions at different ionizer potentials. Jasinski[11] and others have done experiments at lower ionizer potentials (20 eV or less) to reduce the sensitivity of SiH^+ and improve that of SiH_3^+. To ensure accuracy of our results, we repeated a series of experiments in which the production of SiH_x radicals was monitored as the ionizer energy was lowered from 70 to 18.75 eV, the lower value being an instrument limitation. Also, we monitored changes in the argon m/e ratios at 36, 38, and 40 as a function of ionizer potential. Our results from both experiments show a similar trend to those previously obtained [8, 9, 10] but are consistently offset by about 5 eV, possibly due to any of a number of unoptimized parameters including ion optics, bias grids and stretching the operating conditions of the mass spectrometer. See figure 15 for argon data, compared to that obtained by Rapp[10]. Justification for carrying experiments stems from a realization that by 20 eV, the sensitivity of the SiH^+ fragment is very low - almost negligible. At a similar energy, the SiH_3^+ response is still about 60%. Also, due to the low sensitivity of SiH^+ at 20 eV, there is less interference of the silicon-29 isotope as $Si^{29}H$ on the mass 30 ($Si^{28}H_2^+$) signal. The ubiquitous and dominant SiH_2^+ fragment is a result of energetics; it takes least energy for its generation from silane, equation 3.

(3) $SiH_4 \rightarrow SiH_2 + 2\,H$ (f=0.83) 2.2 eV

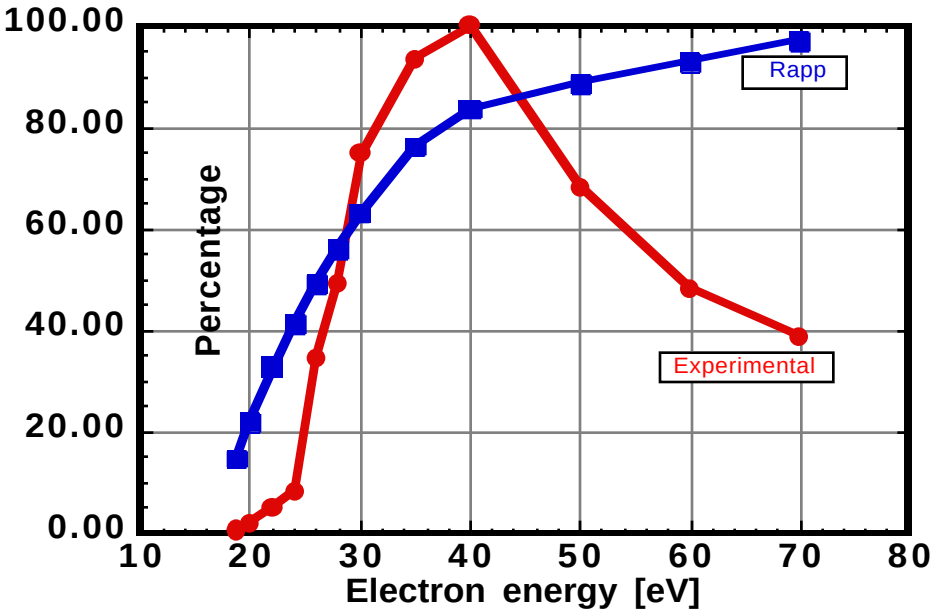
100.00
80.00
60.00
40.00
20.00
0.00
Percentage
10
20
30
40
50
60
70
80
Electron energy [eV]
Rapp
Experimental

Compared to Jasinski[11] whose measurements indicated a substantial amount of SiH_3^+ production, our results show an inverse relation - low amounts of SiH_3 and higher amounts of SiH in the gas phase. Normalized by the m/e 30 signals with and without plasmas, figure 16 shows a larger increase at m/e ratio 29 than at m/e 31. Even though the curves were corrected for background effects, a large peak is still observed at m/e 28, hindering any chance of estimating the intensity due to Si^+.

Providing information about the species present in the gas phase due to plasma excitation and corroborating the mass spectra, a peak at 414 nm corresponding to SiH* radical was always present in the optical emission spectra regardless of silane flow rate during hydrogen plasma discharges. This observation suggests that recycling off the walls is a significant process and must be taken into account. To check this hypothesis, tests were done in which the plasma was kept on without silane into the system. Significant amounts at m/e 29, 30, 31 were observed.

Regarding the mechanism of film growth, reports [17] have been made that attribute the deposition process to SiH_2 insertion in the disilane species, Si_2H_6 and other silane species. Our gas phase results do not reflect the presence of higher order silane species.

As mentioned earlier, the presence of atomic hydrogen has profound effect on the film properties. Figure 17, a plot of the refractive index against the nitrogen-silicon ratio (gas phase) exemplifies the effect of hydrogen. Without hydrogen addition, the refractive index does not change much as a function of gas flow. The introduction of hydrogen in the ionization region increases the processing window and makes possible the fabrication of materials with refractive index greater than 2. In figures 18 and 19, the amount of SiH (mass 29) normalized with respect to SiH_2 is plotted with and without H_2 versus time in which nitrogen flow is changed. With increased nitrogen flow (0 to 20 sccm), the SiH

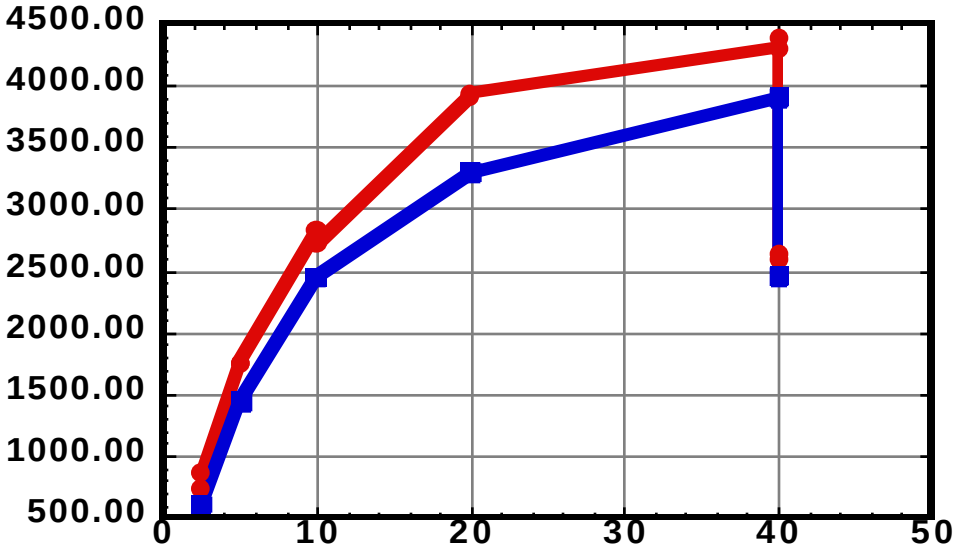
4500.00
4000.00
3500.00
3000.00
2500.00
2000.00
1500.00
1000.00
500.00
0
10
20
30
40
50

amount is correspondingly seen to increase. Both trends with and without hydrogen are similar, with higher SiH amounts in the absence of hydrogen. The following deduction can be made from figures 17 and 18: increasing the N/Si ratio correlates with increased SiH, which also reflects decreasing refractive index. One explanation for this could be that higher SiH amounts lead to more nitrogen incorporation in films, hence nitrogen-rich films - which generally have lower refractive indices than their silicon-rich counterparts. For the case of hydrogen in figure 17, the initial high refractive index (corresponding to being silicon-rich) decreases as the amounts of SiH increase favoring more nitrogen in films. Another reason for the difference in figure 17 can be attributed to the production of atomic hydrogen. This will be discussed later. Also, the lack of change in the refractive index with the no-hydrogen data may be due to oxygen contamination in the films.

The band gap decreases with hydrogen gas addition, shown in figure 20. With hydrogen addition, the goal of films with band gaps greater than 4 eV and refractive indices greater than 2 can still be achieved. The striking difference between the curves can be attributed to the production of atomic hydrogen and the subsequent abstraction of hydrogen in the films. An earlier study[18] simulating the role of hydrogen in silicon nitride films, shows the band gap as being related to the amount of hydrogen incorporation. Dangling bonds are under-coordinated silicon or nitrogen atoms which create localized electronic levels in the band gap. Hydrogen incorporation can passivate the dangling bonds, which would lead to removal of the electronic levels in the band gap, and higher band gaps. This we observe from figure 20, that the band gap values in the absence of H_2 gas - more hydrogen in films - are higher than those made with hydrogen. The dip in the band gap for the no-hydrogen case could be real or could be due to impurities such as oxygen.

As mentioned earlier, one of the goals for this study is to relate gas phase species to film properties. In figure 21, a plot of the percentage change in the SiH_3^+ normalized by SiH_2^+

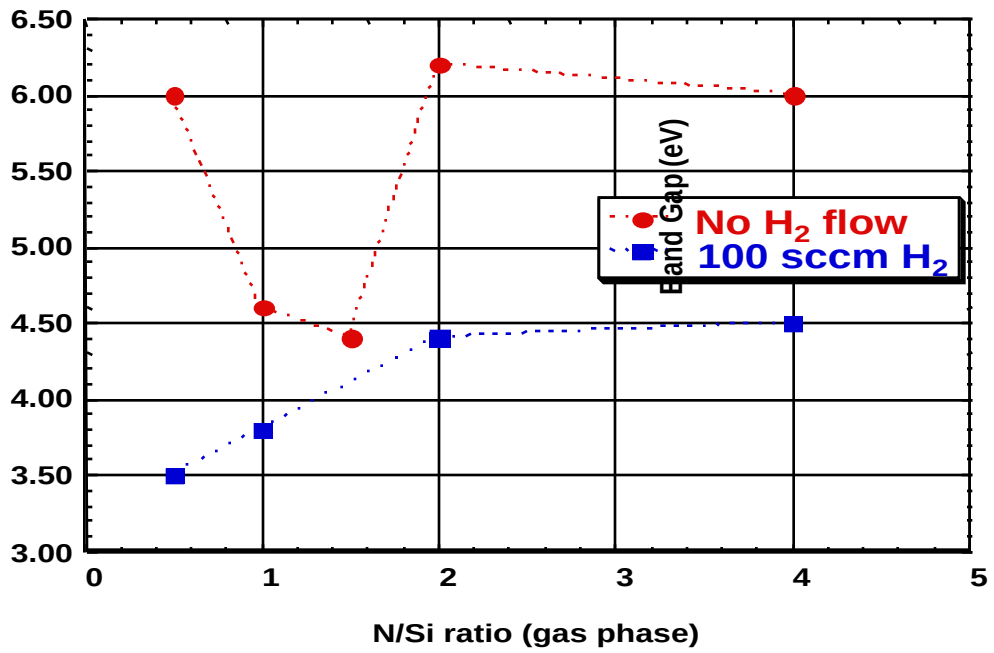

Figure 20: Band gap versus nitrogen-silicon ratio in gas phase; Power=1 kW, 10 sccm SiH_4, Substrate temperature=380 ºC

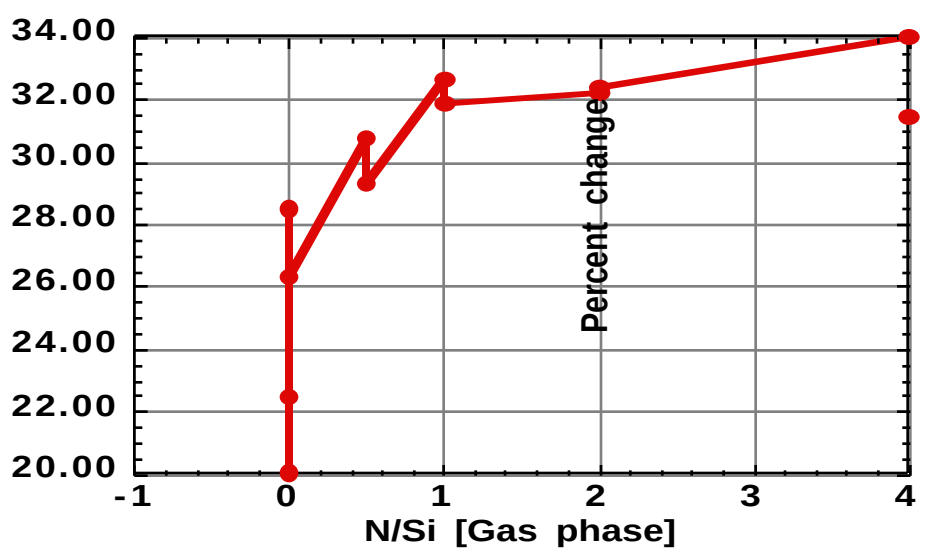

Figure 21: Change in SiH_3/SiH_2 ratio versus nitrogen-silicon ratio in gas phase

response shows a trend similar to the band gap values with hydrogen addition as a function of nitrogen-silicon ratio (figure 20). Initially, both curves increase rapidly, then level off as nitrogen-silicon ratio increases. Tentatively, we observe some correlation between film properties and gas phase species. Similar trends will be investigated for other properties and gas phase species.

Figure 22 shows the effect of atomic hydrogen on the deposition rate of the films. Compared to the case without hydrogen, the presence of atomic hydrogen from the added H_2 gas is responsible for the lower deposition rates. The higher flux of atomic hydrogen etches the film and reduces the deposition rate. With nitrogen addition, the rate (for the H_2 gas addition case) increases and approaches 40 nm/min.

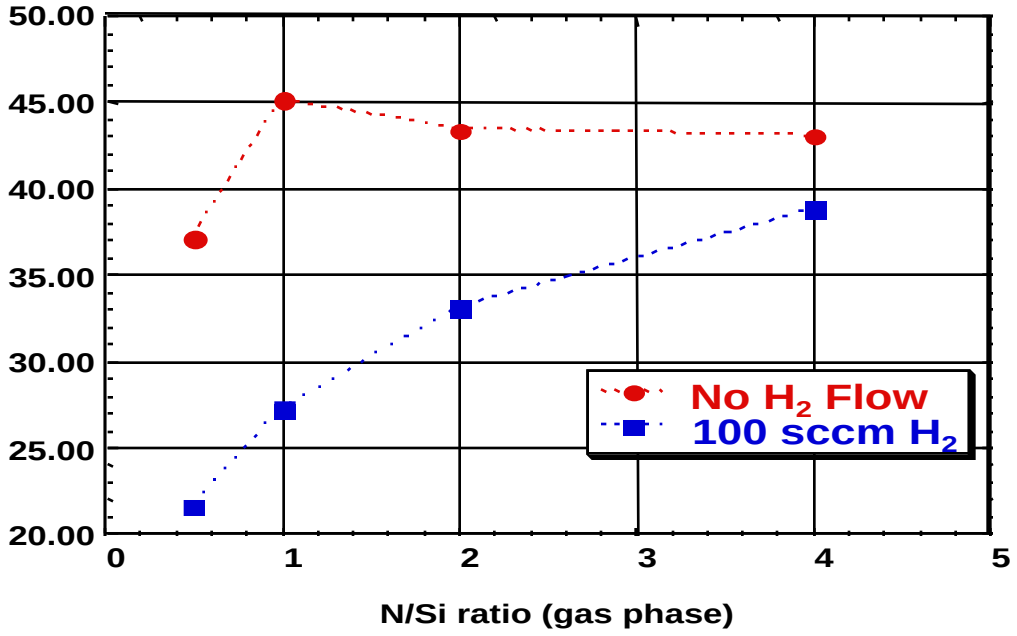

Figure 22: Deposition rate plotted against nitrogen-silicon ratio in gas phase

The no-hydrogen gas films are silicon-rich but addition of hydrogen also allows the Si_3N_4 stoichiometry (N/Si=1.3) to be achieved, confirmed from RBS studies. Hydrogen flow can also reduce other impurities in the films, such as oxygen. This has also been confirmed from RBS, figure 23, thus suggesting that oxygen contamination inhibits the incorporation of nitrogen in the films.

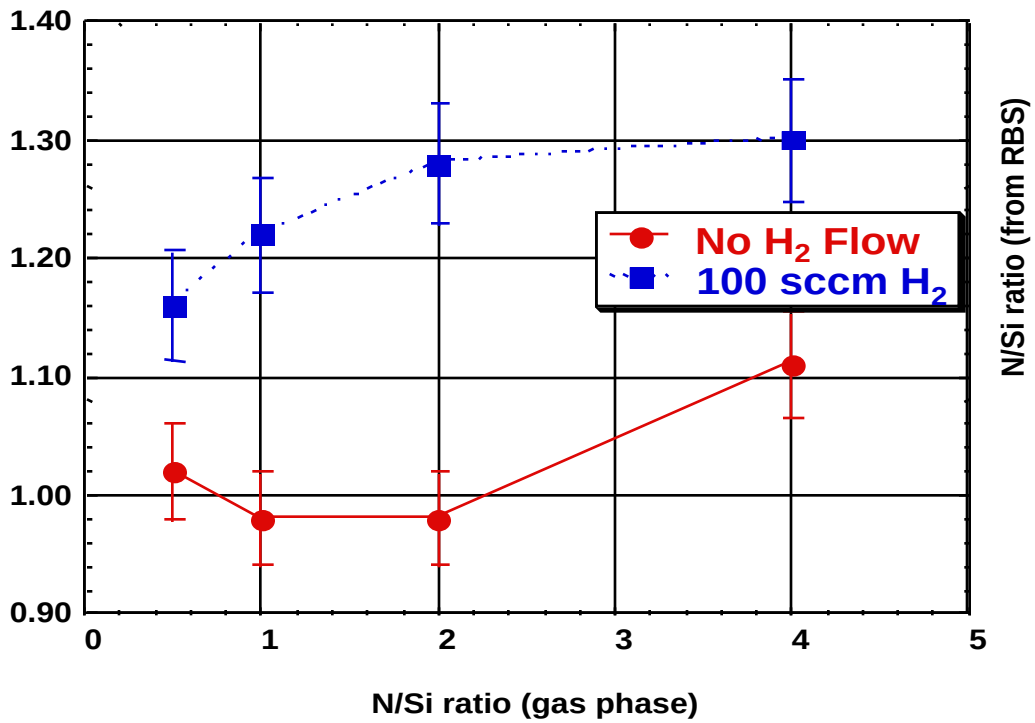

Figure 23: Nitrogen-silicon ratio in film (RBS) versus amount in gas phase; Power=1 kW, Silane flow=10 sccm, Substrate temperature=380ºC

As mentioned earlier, the hydrogen content in the films is reduced when H_2 is added to the plasma. This is consistent with previous work by Parsons[19] showing that presence of atomic hydrogen results in hydrogen abstraction from the silicon-hydrogen surface, ultimately resulting in net reduction of the hydrogen in the films. FTIR results, figures 24 and 25, reveal the N-H stretch is lower with hydrogen flow. The fact that the intensity of the N-H stretch line decreases means that there is less hydrogen in the film. Shown in

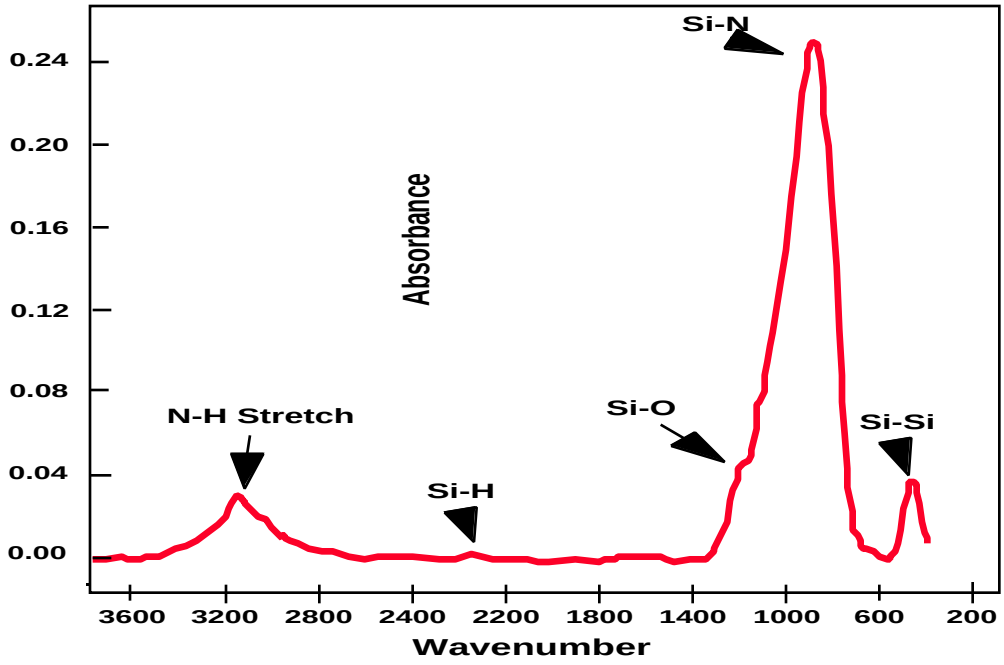

Figure 24: FTIR spectra showing stretching modes in absence of hydrogen

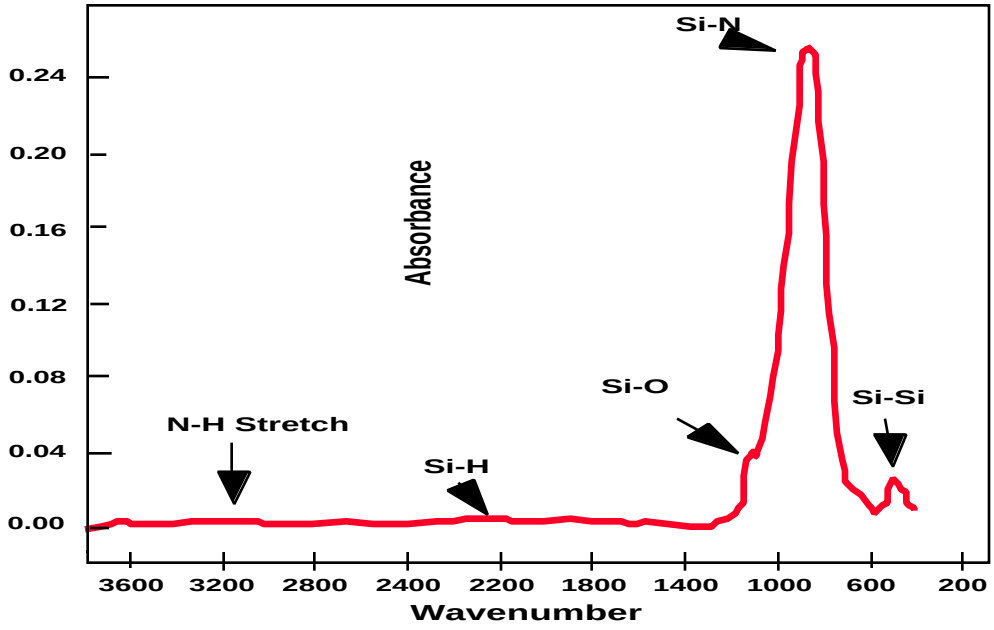

Figure 25: FTIR spectra obtained from a film deposited with 100 sccm H_2, N_2 Flow rate=SiH_4 Flow rate=10 sccm

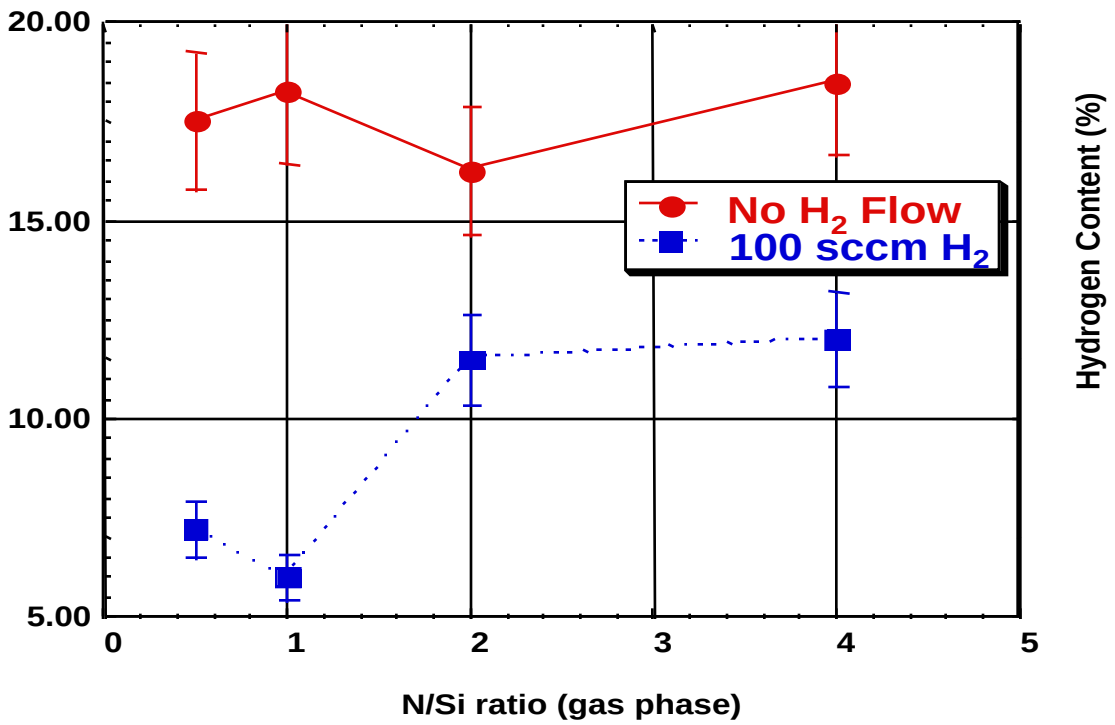

Figure 26: Hydrogen content in films determined using Hydrogen Forward Scattering

SUMMARY

The differences in the species observed using an ICP discharge as opposed to conventional methods might be a result of being in a new processing regime. We observed higher amounts of SiH^+ instead of the SiH_3^+ reported elsewhere[11]. From our results, we did not observe any disilanes or higher order silane species, leading us to conclude they are either below our detection limits or SiH_2^+ is not the primary precursor in our experiments.

Since significant amounts of SiH in the optical emission spectra were observed regardless of the silane flow, we are led to believe that there are more factors other than gas phase reactions at work. These should include either gas phase-wall reactions or the chamber acting as a pump, releasing radicals when heated. Another explanation for the high amounts of SiH observed could be a result of dissociation kinetics. After SiH_3 has been produced, it takes very little energy to further break it down into SiH and H_2.

Addition of hydrogen gas, and the subsequent production of atomic hydrogen, to the plasma increases the processing window and makes the goal of films with refractive indices greater than 2 and band gaps greater than 4 realizable. Also, our deposition rates (20 - 45 nm/min) are due to the higher dissociation of the diatomics, ultimately leading to a higher flux of atomic species and higher utilization of silane.

Tentatively, we have found a correlation between the change in SiH_3^+/SiH_2^+ production and the band gaps obtained with hydrogen addition. However, it must be pointed out that this work is in progress, interpretation may be subject to change pending review and analysis of results.

REFERENCES

1. F. de Brito Mota, J.F. Justo, and A. Fazzio, “Structural properties of amorphous silicon nitride,” Phys. Rev. B **58** (13), 1 October 1998, pp. 8323 - 8328.

2. T.M Klein, T.M. Anderson, A.I. Chowdhury, and G.N. Parsons, “Hydrogenated silicon nitride thin films deposited between 50 and 250 C using nitrogen/silane mixtures with helium dilution,” J. Vac. Sci. Technol. A **17** (1), January/February 1999, pp. 108 - 112.

3. “Plasma deposited thin films,” edited by J. Mort and F. Jansen, (CRC Press, Florida, 1986).

4. J. Caughman, G. Bell, D. Beach, S. Gorbatkin, “Advanced deposition techniques for producing thin films of polycrystalline silicon,”

5. L.S. Zambom, R.D. Mansano, R. Furlan, P. Verdonck, “LPCVD deposition of silicon nitride assisted by high density plasmas,” Thin Solid Films **343-344**, 1999, pp. 299 - 301.

6. M. Maeda and H. Nakamura, “Infrared spectroscopic study of hydrogenated and deuterated silicon nitride films prepared from plasma-enhanced deposition,” J. Appl. Phys. **55** (8), 15 April 1984, pp. 3068 - 3071.

7. J. Tersoff, “Structural properties of sp3-bonded hydrogenated amorphous carbon,” Phys. Rev. B, **44**, 1991, pp. 12039.

8. R. Basner, M. Schmidt, V. Tarnovsky, K. Becker, H. Deutsch, “Dissociative ionization of silane by electron impact,” International Journal of Mass Spectrometry and Ion Processes **171**, 1997, pp. 83 - 93.

9. E. Krishnakumar and S.K. Srivastava, “Ionization cross sections of silane and disilane by electron impact,” Contrib. Plasma. Phys. **35**, 1995, pp. 395 - 405.

10. D. Rapp and P. Englander-Golden, “Total cross sections for the ionization and attachment in gases by electron impact,” J. Chem. Phys. **43** (5), 1 September 1965, pp. 1464 - 1479.

11. J.M. Jasinski, “Mass spectrometric studies of remote helium plasma dissociation of silane,” J. Vac. Sci. Technol. A **13** (4), Jul/Aug 1995, pp.1935 - 1940.

12. H. Chatham, D. Hills, R. Robertson, and A. Gallagher, “Total and partial electron collisional ionization cross sections for CH4, C2H6, SiH4, and Si2H6,” J. Chem. Phys. **81** (4), 15 August 1984, pp. 1770.

13. M.J. Kushner, “Simulation of the gas-phase processes in remote-plasma-activated chemical-vapor deposition of silicon dielectrics using rare gas-silane-ammonia mixtures,” J. Appl. Phys. **71** (9), 1 May 1992, 99. pp. 4173.

14. D.C. Marra, E.A. Edelberg, R.L. Noane, E.S. Aydil, “Silicon hydride composition of plasma-deposited hydrogenated amorphous and nanocrystalline silicon films and surfaces,” J Vac. Sci. Technol. **16**, 1998, pp. 3199.

15. J.R. Doyle, D.A. Doughty, and A. Gallagher, “Silane dissociation products in deposition discharges,” J. Appl. Phys. **68** (9), 1 November 1990, pp. 4375 - 4384.

16. S. Ramalingam, D. Maroudas, E.S. Aydil, “Interactions of SiH radicals with silicon surfaces: An atomic-scale simulation study,” J. App. Phys. **84** (7), 1998, pp. 3895.

17. F.J. Kampas and R.W. Griffith, “Hydrogen elimination during the glow-discharge deposition of *a*-SiH alloys,” Appl. Phys. Lett. **39**, 1981, pp. 407.

18. F. de Brito Mota, J.F. Justo, and A, Fazzio, “Hydrogen role on the properties of amorphous silicon nitride,” J. Appl. Phys. **86** (4), 15 August 1999, pp. 1843 - 1847.

19. E. Srinivasan and G.N. Parsons, “Hydrogen abstraction kinetics and crystallization in low temperature plasma deposition of silicon,” Appl. Phys. Lett. **72** (4), 1 January 1998, pp. 456 - 458.